Cole-Cole law for critical dynamics in glass-forming liquids

Matthias Sperl
Department of Physics, Duke University, Box 90305, Durham, North Carolina 27708, USA
(Received 19 February 2006; published 13 July 2006)

Within the mode-coupling theory (MCT) for glassy dynamics, the asymptotic low-frequency expansions for the dynamical susceptibilities at critical points are compared to the expansions for the dynamic moduli; this shows that the convergence properties of the two expansions can be quite different. In some parameter regions, the leading-order expansion formula for the modulus describes the solutions of the MCT equations of motion outside the transient regime successfully; at the same time, the leading- and next-to-leading-order expansion formulas for the susceptibility fail. In these cases, one can derive a Cole-Cole law for the susceptibilities; and this law accounts for the dynamics for frequencies below the band of microscopic excitations and above the high-frequency part of the α peak. It is shown that this scenario explains the optical-Kerr-effect data measured for salol and benzophenone (BZP). For BZP it is inferred that the depolarized light-scattering spectra exhibit a wing for the α peak within the Gigahertz band. This wing results from the crossover of the von Schweidler law part of the α peak to the high-frequency part of the Cole-Cole peak; and this crossover can be described quantitatively by the leading-order formulas of MCT for the modulus.

DOI: 10.1103/PhysRevE.74.011503 PACS number(s): 61.20.Lc, 82.70.Dd, 64.70.Pf

I. INTRODUCTION

During the past 15 years, several new spectrometers have been introduced for the study of the glassy dynamics of liquids. The evolution of this complex slow dynamics upon decreasing the temperature T or increasing the density ρ has been documented for many systems for times t, which exceed the natural time scale t_{mic} for condensed-matter motions by three or more orders of magnitude. Similar progress has been made for molecular-dynamics simulations of liquid models. In parallel to these experimental activities, a theory for the evolution of glassy dynamics has been developed which is referred to as mode-coupling theory (MCT). This theory is based on regular equations of motion for a set of autocorrelation functions. The MCT equations lead to fold bifurcations for the correlators' long-time limits if some control parameter like T reaches a critical value T_c; this bifurcation describes a transition from a liquid to an amorphous solid. The distance of the control parameter from the critical value, say $\varepsilon=(T_c-T)/T_c$, can be used for the discussion of the bifurcation dynamics as a small parameter. For ε tending to zero and times increasing to infinity, it is possible to calculate asymptotic solutions of the MCT equations. The leading-order results provide a set of general formulas, which explain the qualitative features of the bifurcation scenario. Many fits of data with these general formulas have been studied in order to test the relevance of the MCT for the explanation of the experimental facts [1].

A set of general MCT results, which is of main interest in this paper, concerns the critical dynamics. This dynamic is described by autocorrelation functions $\phi(t)$ for control parameters at the bifurcation point, say $T=T_c$. Equivalently, one can consider the corresponding loss spectra $\chi''(\omega)$. These are the products of the frequency ω and the Fourier-cosine transform of $\phi(t)$. The central asymptotic formula is specified by (1) a positive number f^c, which is called the plateau, (2) a positive amplitude, say A, and (3) the critical exponent a, obeying $0<a<0.396$, $\lim_{t\to\infty} t^a[\phi(t)-f^c]=A$. This formula is equivalent to $\lim_{\omega\to 0}\chi''(\omega)/\omega^a=\sin(\pi a/2)\Gamma(1-a)A$, with Γ denoting the gamma function. For a given transition point, all correlators are specified by the same exponent a, but different critical points can differ in their value for a. The leading-order long-time result for the correlator describes a power-law decay, $\phi(t)-f^c\propto 1/t^a$. Equivalently, the leading-order result for the low-frequency critical loss spectrum is given by a power-law variation $\chi''(\omega)\propto\omega^a$. For states near the transition point, $\phi(t)$ and $\chi''(\omega)$ can be replaced by their respective critical functions for short times, $t\ll t_\sigma$, or large frequencies, $\omega t_\sigma\gg 1$. The time scale t_σ is the same for all correlators and diverges for states approaching the transition point. For $t\geqslant t_\sigma$ and $\omega t_\sigma\leqslant 1$, the correlators and spectra depend sensitively on ε; for shorter times, $t\ll t_\sigma$ and $\omega t_\sigma\gg 1$, the correlators and spectra depend on ε smoothly. An ω^a spectrum was identified first for the glass-forming molten salt $0.4\mathrm{Ca}(\mathrm{NO}_3)_2 0.6\mathrm{K}(\mathrm{NO}_3)$ (CKN) in data obtained by neutron-scattering spectroscopy [2]. This system was also used to document for the first time the evolution of glassy dynamics within the full Giga-Hertz band [3]: Using depolarized light-scattering spectroscopy, a spectrum compatible with the ω^a law was found extending from 1 GHz to 400 GHz. The t^{-a} decay in the time domain was measured first for density correlators by photon-correlation spectroscopy for a colloidal suspension of hard spheres [4] with the density as a control parameter.

Other glass-forming systems that can be studied experimentally are found in many van der Waals liquids. The natural time scale for intermolecular vibrations is a picosecond. For normal liquid behavior, one expects correlations to decay to zero for times around some picoseconds. The normal-liquid excitation spectra extend from, say, 0.5 THz to, say, 5 THz. Glassy-dynamics spectra for several systems have been measured by depolarized light-scattering spectroscopy, and the data were shown to be consistent with the MCT bifurcation scenario. For example, spectra for toluene have been fitted successfully with leading-order asymptotic results for frequencies between 0.5 GHz and 1 THz and for tem-

peratures decreasing from $T=T_c+140$ K to T_c+10 K; $T_c \approx 150$ K [5]. For all these systems, the weight of the glassy dynamics part of the spectra is large compared to the part of normal-liquid dynamics, i.e., the so-called α peak is large. In agreement with the MCT prediction for such situations, the amplitude A for the ω^a spectrum is small, and the low-frequency contributions of the normal-liquid dynamics affect the region of the expected ω^a behavior of the spectra. As a result, no frequency interval has ever been identified for a van der Waals liquid, where an ω^a spectrum can be identified explicitly.

Torre *et al.* [6] have introduced optical-Kerr-effect (OKE) spectroscopy as a technique for the study of glassy dynamics. The measurement provides the response function $\chi(t) \propto -\partial_t \phi(t)$ for the same probing variable, which is studied in depolarized light-scattering experiments. The Fourier-sine transforms of $\chi(t)$ are proportional to the loss spectra $\chi''(\omega)$ mentioned in the preceding paragraph. The evolution of the glassy dynamics of *m*-toluidine was measured for temperatures decreasing from 295 K to 250 K. The response functions could be fitted well by the scaling-law results predicted by the leading-order asymptotic formulas for the MCT bifurcation [7]. The analysis implies a critical temperature T_c near 220 K and a critical exponent a near 0.3. However, lowering the temperature to 225 K, the critical power-law decay $\chi(t) \propto 1/t^{1+a}$ was not observed [8]. The negative slope of the measured log χ-versus-log t curve is not $1+a$, rather it is a number smaller than unity, say $1-b'$. Decay laws $\chi(t) \propto 1/t^{1-b'}$ with exponents b' around 0.2 have been identified by Cang *et al.* [9] for a number of other van der Waals liquids. The OKE response of salol was studied by Hinze *et al.*, and the data were shown to be consistent with the known MCT scaling law formulas for the temperature decreasing from 340 K to 266 K [10]. The glassy response for $T=257$ K was measured with an impressive accuracy for times increasing up to 0.5 μs; and the dynamics for $t>100$ ps displays the behavior expected from the leading-order asymptotic results of MCT. However, the glassy dynamics for 2 ps$<t<$20 ps manifests itself by a $\chi(t) \propto 1/t$ decay. The corresponding correlator shows a logarithmic time dependence. All OKE response functions measured so far demonstrate a glassy dynamics that cannot be described by the general leading-order asymptotic formulas for the MCT bifurcation in the regime $t \lesssim 30$ ps. In a recent alternative approach [11] is was possible to fit some of the OKE data for $t>30$ ps.

It was argued recently that the new facets of glassy dynamics discovered by OKE spectroscopy [8–10] can be understood as generic implications of the Cole-Cole law for the critical dynamics [12]. In the following, this statement shall be explained in detail. Section II summarizes the equations of motion and the known scaling-law results of MCT. It is explained in Sec. III that an asymptotic expansion of the modulus can have a much larger range of validity than the expansion for the susceptibility; the Cole-Cole law—introduced in 1941 as empirical law [13]—is derived in full generality from the microscopic equations of motion. The relevance of these results is demonstrated for a schematic model in Sec. IV using parameter values that describe the mentioned OKE data. The interplay between the Cole-Cole peak and the α-peak is investigated in Sec. V where for specific parameter values the α peak displays a wing. Section VI presents a conclusion.

II. ESSENTIAL MCT FORMULAS

A. Equations of motion

Within the basic version of MCT, the dynamics of the system is described by M correlators $\phi_q(t)$, $q=1,\ldots,M$. These are real and even functions of the time t, which obey the initial conditions $\phi_q(t=0)=1$, $\partial_t \phi_q(t=0)=0$. The corresponding set of normalized response functions is given by

$$\chi_q(t) = -\partial_t \phi_q(t). \tag{1a}$$

Laplace transforms map functions from the time domain, say $F(t)$, in the frequency domain. They shall be used with the convention $\mathrm{LT}[F(t)](z)=i\int_0^\infty dt \exp(izt)F(t)$, $z=\omega+i0$. One gets $\mathrm{LT}[\chi_q(t)](z)=[1+\omega\phi_q(\omega)]$, where $\phi_q(\omega)=\mathrm{LT}[\phi_q(t)](z)$. The normalized dynamical susceptibilities are given by

$$\chi_q(\omega) = 1 + \omega\phi_q(\omega). \tag{1b}$$

The loss spectra $\chi_q''(\omega)=\mathrm{Im}\,\chi_q(\omega)$ are related trivially to the fluctuation spectra $\phi_q''(\omega)=\mathrm{Im}\,\phi_q(\omega)$: $\chi_q''(\omega)=\omega\phi_q''(\omega)$.

The Zwanzig-Mori formalism provides a fraction representation of $\phi_q(\omega)$ in terms of a fluctuating-force correlator $M_q(\omega)$: $\phi_q(\omega)=-1/\{\omega-\Omega_q^2/[\omega+M_q(\omega)]\}$. The positive frequency Ω_q quantifies the initial decay of the correlator $\phi_q(t)=1-(\Omega_q t)^2/2+\mathcal{O}(t^3)$. Within MCT, a white-noise term ν_q is split off from the kernel $M_q(\omega)$; the remainder is represented in terms of a dimensionless function $m_q(t)$: $M_q(\omega)=i\nu_q+\Omega_q^2 m_q(\omega)$; $\nu_q \geqslant 0$. Here, $m_q(t)$ and $m_q(\omega)$ are related by Laplace transformation. The fraction representation is equivalent to the equations of motion

$$\partial_t^2 \phi_q(t) + \nu_q \partial_t \phi_q(t) + \Omega_q^2 \left(\phi_q(t) + \int_0^t dt' m_q(t-t') \partial_{t'} \phi_q(t') \right) = 0. \tag{2a}$$

The essential approximation in MCT is the expression of $m_q(t)$ as a polynomial $\mathcal{F}_q$ of the correlators

$$m_q(t) = \mathcal{F}_q[\phi_1(t), \ldots, \phi_M(t)]. \tag{2b}$$

There is no monomial contribution of order zero. The coefficients of the polynomial are called mode-coupling coefficients. They are the coupling constants of the theory and must not be negative. Within the microscopic theory, the polynomials are of second order and the coefficients are given by the equilibrium structure functions, which in turn are smooth functions of control parameters like the temperature T for the states considered.

At the generic transition mentioned in the preceding section, the correlator's long-time limits depend singularly on the distance parameter ε. For $\varepsilon<0$, fluctuations disappear for long times, $\phi_q(t\to\infty)=0$. For $\varepsilon \geqslant 0$, $\phi_q(t\to\infty)=f_q$, $0<f_q<1$, $q=1,\ldots,M$; the fluctuations arrest. Within the microscopic version of MCT, the arrested part f_q has the

meaning of the Debye-Waller factor of the solid amorphous state. The leading-order variation with changes of ε for the arrested part is given by $f_q - f_q^c \propto \sqrt{\varepsilon}$, $\varepsilon \to 0^+$, $f_q^c > 0$, $q = 1, \ldots, M$. The regularity of the MCT equations implies the following. For ε tending to arbitrarily small values, there appears an arbitrarily large time interval, where $\phi_q(t)$ is arbitrarily close to f_q^c. This critical arrested part f_q^c has the meaning of a plateau for the $\phi_q(t)$-versus-log t curves for states near the transition. The corresponding plateau for the force correlators is $m_q(t \to \infty) = f_q^{mc} = \mathcal{F}_q^c(f_1^c, \ldots, f_M^c)$. At the transition, $\phi_q(\omega)$ and $m_q(\omega)$ exhibit poles $-f_q^c/\omega$ and $-f_q^{mc}/\omega$, respectively. Hence, there is a region of small $|\varepsilon|$ and small ω, where $\omega + i\nu_q$ can be neglected compared to $\Omega_q^2 m_q(\omega)$. This region is the one for the MCT glassy dynamics. The fraction representation of the correlators simplifies to $\phi_q(\omega) = -1/[\omega - 1/m_q(\omega)]$. This formula can also be noted as

$$\omega m_q(\omega) = \omega \phi_q(\omega)/[1 + \omega \phi_q(\omega)]. \tag{3a}$$

Equation (1b) yields the equivalent expression for the dynamical susceptibility

$$\chi_q(\omega) = 1/[1 - \omega m_q(\omega)]. \tag{3b}$$

Within the regime of glassy dynamics, $[1 - \omega m_q(\omega)]$ has the meaning of a modulus for the response described by $\chi_q(t)$. The pair of Eqs. (2b) and (3a) can fix the solution only up to some overall time scale t_0. The latter is determined by matching of the transient dynamics with the glassy dynamics. For further details and for a list of original papers, the reader can consult Ref. [14].

B. Scaling laws

There is a straightforward recipe to calculate from the coupling coefficients at the transition point and from the critical arrested parts f_q^c a number λ, $1/2 \leq \lambda < 1$. It is called the exponent parameter for the chosen transition point of the model under discussion. It fixes the critical exponent a, mentioned in Sec. I. It fixes a further exponent b, $0 < b \leq 1$, which is called the von Schweidler exponent. The equation for the two exponents reads $\Gamma(1-a)^2/\Gamma(1-2a) = \lambda = \Gamma(1+b)^2/\Gamma(1+2b)$. Parameter λ also specifies a pair of equations for a pair of functions $g_\pm(\hat{t})$, which are defined for $\hat{t} > 0$. The equations read $\pm 1 + \lambda g_\pm(\hat{t})^2 = (d/d\hat{t}) \int_0^{\hat{t}} d\hat{t} g_\pm(\hat{t} - \hat{t}') g_\pm(\hat{t}')$, and they must be solved with the initial condition $\lim_{\hat{t} \to 0} \hat{t}^a g_\pm(\hat{t}) = 1$. Up to corrections of order $\hat{t}^a$, one gets for small $\hat{t}$,

$$g_\pm(\hat{t} \ll 1) = 1/\hat{t}^a. \tag{4a}$$

The function $g_+(\hat{t})$ approaches its long-time limit exponentially, $g_+(\hat{t} \gg 1) = 1/\sqrt{1-\lambda}$. The function $g_-(\hat{t})$ exhibits a power-law divergence for large $\hat{t}$. Up to corrections of order $1/\hat{t}^b$, one gets

$$g_-(\hat{t} \gg 1) = -B\hat{t}^b. \tag{4b}$$

There are tables allowing the determination of a, b, and B from a given λ. There are also tables to determine $g_\pm(\hat{t})$ with an accuracy sufficient for all practical purposes [15].

The functions $g_\pm(\hat{t})$ are the shape functions for the first scaling law of MCT. For ε tending to zero, there appears a time interval of diverging length, within which $\Delta_q(t) = |\phi_q(t) - f_q^c|$ is arbitrary small. The leading-order solution for the small parameter $\Delta_q(t)$ yields the first scaling law. The solution assumes the form

$$\phi_q(t) = f_q^c + h_q \sqrt{|\sigma|} g_\pm(t/t_\sigma), \quad \varepsilon \gtrless 0. \tag{5a}$$

The amplitudes $h_q > 0$, $q = 1, \ldots, M$ are calculated from the mode-coupling coefficients at the critical point. The separation parameter σ is defined similarly: it is a smooth function of the control parameters and can be linearized close to the transition point, $\sigma = C\varepsilon + \mathcal{O}(\varepsilon^2)$, with a positive coefficient C that depends on the chosen control parameter. The first critical time scale t_σ is given by the critical exponent a, the separation parameter σ, and the time scale t_0, which is defined by the short-time dynamics,

$$t_\sigma = t_0/|\sigma|^\delta, \quad \delta = 1/(2a). \tag{5b}$$

The strong control-parameter dependence of the correlators near the plateau is described solely by that of the correlation scale $\sqrt{|\sigma|}$ and of the time scale t_σ.

From Eqs. (4a), (5a), and (5b), one gets the leading-order asymptotic law for the decay of the critical correlator discussed in Sec. I, $\phi_q(t) - f_q^c = h_q(t_0/t)^a$. From Eqs. (4a), (5a), and (5b) one gets the von Schweidler law for the decay of the liquid correlators below the plateau,

$$\phi_q(t) = f_q^c - h_q(t/t_{\sigma'})^b, \quad t_\sigma \ll t \ll t_{\sigma'}, \quad \varepsilon < 0. \tag{6}$$

Here, the second critical time scale of MCT reads $t_{\sigma'} = t_0/(B^{1/b}|\sigma|^\gamma)$, with $\gamma = 1/(2a) + 1/(2b)$. Up to errors of order $|\varepsilon|$, the decay of the liquid correlators below the plateau is described by the second scaling law of MCT

$$\phi_q(t) = \tilde{\phi}_q(t/t'_\sigma), \quad t'_\sigma \ll t, \quad \varepsilon < 0. \tag{7}$$

Here, $\tilde{\phi}_q(\tilde{t})$ is an ε-independent shape function. Its initial part is given by von Schweidler's law: $\tilde{\phi}_q(\tilde{t} \ll 1) = f_q^c - h_q \tilde{t}^b$. Corrections of order $\sqrt{|\varepsilon|}$ modify the formula (7) for the below-plateau decay in a regime where $\phi_q(t)$ is close to the plateau. These corrections are described by Eq. (5a) for $t \gtrsim t_\sigma$. The below-plateau decay is referred to as α process, and Eq. (7) formulates the superposition principle. Details of the derivation of the cited results, references to the original work, and a comprehensive demonstration for the hard-sphere system can be found in Refs. [14,16].

III. CRITICAL DYNAMICS AND COLE-COLE LAW

In this section, correlators and susceptibilities shall be discussed for states at the transition point, say $T = T_c$. Focusing on the range of validity, the essential formulas are analyzed for the correlators in Sec. III A, and for the susceptibilities in Sec. III B. The Cole-Cole law is derived in Sec. III C.

A. Power-law solution for correlation functions

The leading-order scaling-law formulas (4a) and (5a) yield for the critical correlators

$$\phi_q(t) = f_q^c + h_q(t_0/t)^a. \tag{8}$$

A first question, whose answer is not implied by the results cited in Sec. II B, concerns the range of validity of Eq. (8) for short times. Let us define an onset time t_q^* for the power law by the request, that Eq. (8) describes $\phi_q(t) - f_q^c$ within a relative error of, say, 10%, for $t \geq t_q^*$. For normal-liquid dynamics, one would expect the correlators to decay to zero for times around t_{mic}. A second question to be discussed is: How can one describe the critical correlators in cases where t_q^* exceeds t_{mic}, i.e., when there is a gap between the end of the transient regime and the onset of the critical power law?

The asymptotic solution (8) can be extended to an asymptotic series expansion in powers of t^{-a}. The result up to the next-to-leading term shall be noted as

$$\phi_q(t) = f_q^c + h_q(t_0/t)^a[1 + \hat{K}_q(t_0/t)^a]. \tag{9a}$$

Here, remainders which are given by $(t_0/t)^{3a}$ times some power of $\ln(t/t_0)$ are dropped. The Tauberian theorem yields an equivalent formula in the frequency domain,

$$\omega\phi_q(\omega) = -f_q^c - \Gamma(1-a)h_q(-i\omega t_0)^a - \Gamma(1-2a)h_q\hat{K}_q(-i\omega t_0)^{2a}. \tag{9b}$$

In this formula, terms are dropped, which are proportional to ω^{3a} times some power of $\ln \omega$. The preceding two formulas are the starting point for the following derivations. It is a straightforward procedure to calculate the correction amplitude $\hat{K}_q$ from the mode-coupling coefficients at the critical point $T = T_c$ [14]. From Eq. (9a), one can estimate an onset time of $t_q^*/t_0 = (10|\hat{K}_q|)^{1/a}$. This is an estimate based on the assumption that higher-order expansion terms in Eq. (9a) do not influence the results seriously for $t \geq t_q^*$. Typically for many systems, the critical exponent a is around 0.3, and $1/a \gtrsim 3$. Hence, t_q^* depends sensitively on the correction amplitude $\hat{K}_q$. As a result, t_q^* can vary considerably for different q. As a relevant example, let us cite the results for the density-fluctuation correlators of a system of hard spheres of diameter d [14]: The time t_1^* referring to a wave number $q_1 d = 7.0$ exceeds the time t_2^* for $q_2 d = 10.6$ by a factor of around 100.

B. Power-law solution for the susceptibilities

From Eqs. (1a) and (8), one obtains the long-time result for the response functions up to leading-order corrections,

$$\chi(t)t_0 = a h_q(t_0/t)^{1+a}. \tag{10}$$

According to Eq. (9a), the leading order result in Eq. (8) is valid for $t \geq t_q^*$, but the onset time for Eq. (10) is later, $t \geq t_q^* 2^{1/a}$, where typically $2^{1/a} \approx 10$. Hence, the detection of the critical dynamics in its leading asymptotic form is more difficult for the response functions than for the correlators.

From Eq. (9b), one arrives at the expansion formula for the absorptive part of the dynamical susceptibility,

$$\chi_q''(\omega) = [\Gamma(1-a)\sin(\pi a/2)]h_q(\omega t_0)^a \times [1 + k_a\hat{K}_q(\omega t_0)^a], \tag{11a}$$

$$k_a = 2\Gamma(1-a)\cos(\pi a/2)/\lambda. \tag{11b}$$

The leading-order power-law result reads

$$\chi_q''(\omega) = [\Gamma(1-a)\sin(\pi a/2)]h_q(\omega t_0)^a, \tag{11c}$$

which has an onset frequency of $\omega_q^* = 1/(t_q^* k_a^{1/a})$; for $\omega \leqslant \omega_q^*$, the leading-order result in Eq. (11c) describes the critical spectrum with an error smaller than 10%. If λ decreases from 1 to 1/2, k_a increases from 2 to near 5. For λ near a typical value of 0.7, k_a is above 3, and the onset frequency for the ω^a law is about 30 times smaller than $1/t_q^*$. Therefore, the detection of the critical power-law in the loss spectra is even more difficult than in the response function.

Including the leading-correction terms in the asymptotic formulas, as noted in Eqs. (9a) and (11a), is an obvious manner to extend the range of applicability of the analytic description of the dynamics. This is demonstrated comprehensively for the MCT for the hard-sphere system in Refs. [14,16]. But there are cases, where this procedure does not lead to satisfactory results. The mean-squared displacement is an example, where the description of the increase towards the plateau by the analog of Eq. (9a) cannot account for the glassy dynamics [16].

C. The Cole-Cole law

Equation (9b) is an asymptotic expansion in terms of powers of the small quantity $\xi = (-i\omega t_0)^a$ that holds up to errors of ξ^3. Substitution of this expansion into Eq. (3a) provides an analogous expansion for $\omega m_q(\omega)$. Let us indicate the nontrivial parts of the coefficients by a superscript m,

$$-\omega m_q(\omega) = f_q^{mc} + \Gamma(1-a)h_q^m(-i\omega t_0)^a + \Gamma(1-2a)h_q^m\hat{K}_q^m(-i\omega t_0)^{2a}. \tag{12}$$

Comparing coefficients of equal powers of ξ, one finds

$$f_q^{mc} = f_q^c/(1-f_q^c), \quad f_q^c = f_q^{mc}/(1+f_q^{mc}), \tag{13a}$$

$$h_q^m = h_q/(1-f_q^c)^2, \quad h_q = h_q^m/(1+f_q^{mc})^2, \tag{13b}$$

$$\hat{K}_q^m = \hat{K}_q + \lambda[h_q/(1-f_q^c)], \quad \hat{K}_q = \hat{K}_q^m - \lambda[h_q^m/(1+f_q^{mc})]. \tag{13c}$$

Since the autocorrelation functions are normalized, $\phi_q(t=0) = 1$, one gets $f_q^c < 1$. The kernel $m_q(t=0)$ can have any positive value. Therefore, in principle, f_q^{mc} can be any positive number. The different normalizations can be eliminated in the critical amplitudes by comparing the ratios h_q/f_q^c and h_q^m/f_q^{mc}:

$$(h_q^m/f_q^{mc}) = (h_q/f_q^c)/(1-f_q^c). \tag{14}$$

These ratios determine the relative amplitude of the dynamics around the plateau within the first scaling-law regime. Equation (5a) yields $[\phi_q(t) - f_q^c]/f_q^c = (h_q/f_q^c)\sqrt{|\sigma|}g_\pm(t/t_\sigma)$, and a corresponding identity holds for $m_q(t)$. From Eq. (14) one concludes that the relative amplitude of the first-scaling-law contribution is larger by $1/(1-f_q^c) > 1$ for the modulus than

for the susceptibility; and $1/(1-f_q^c)$ increases with f_q^c, the α-peak contribution of the loss spectrum. Consequently, within the range of validity of the first scaling law, it is easier to measure the first-scaling-law contribution for the modulus than that for the susceptibility.

The expansion (12) can be substituted into Eq. (3b) in order to obtain an asymptotic expansion for the inverse of the critical susceptibility, i.e., for the modulus. The result shall be noted in the form

$$\chi_q(\omega) = \chi_{0q}^{cc}/[1 + (-i\omega/\omega_q^c)^a + \hat{K}_q^{cc}(-i\omega/\omega_q^c)^{2a}]. \quad (15)$$

The expression $\chi_q(\omega)^{-1}$ is correct up to errors of the order ω^{3a}. The three parameters specifying this formula can be expressed in terms of the coefficients in Eq. (12) and, via Eqs. (13), in terms of the coefficients specifying the correlators in Eq. (9a). One gets $\chi_{0q}^{cc}=1/(1+f_q^{mc})$. This amplitude is the complement of the α-peak strength f_q^c of the normalized loss spectrum,

$$\chi_{0q}^{cc} = 1 - f_q^c. \quad (16a)$$

The characteristic frequency entering the new formula for the susceptibility, is given by $(\omega_q^c t_0)^a=(1+f_q^{mc})/[h_q^m\Gamma(1-a)]$ or by

$$\omega_q^c t_0 = \{(1-f_q^c)/[h_q\Gamma(1-a)]\}^{1/a}. \quad (16b)$$

The correction amplitude reads $\hat{K}_q^{cc}=\hat{K}_q^m(1+f_q^{mc})/(\lambda h_q^m)$, which is equivalent to

$$\hat{K}_q^{cc} = 1 + [(1-f_q^c)/h_q]\hat{K}_q/\lambda. \quad (16c)$$

If the frequencies are so small that $|\hat{K}_q^{cc}(-i\omega/\omega_q^c)| \ll 1$, Eq. (15) simplifies to the transparent expression of the Cole-Cole law,

$$\chi_q(\omega) = \chi_{0q}^{cc}/[1 + (-i\omega/\omega_q^c)^a]. \quad (17)$$

The condition of validity for this formula means that the critical modulus can be described by the simple power law in the first line of Eq. (12). The modulus spectrum obeys a formula analog to Eq. (11c): $\omega m_q''(\omega) = \Gamma(1-a)\sin(\pi a/2)h_q^m(\omega t_0)^a$. Using the 10% criterion from above, the last term in Eq. (12) can be dropped for frequencies $\omega t_0 \leqslant \{\lambda/[10\Gamma(1-a)|\hat{K}_q^m|]\}^{1/a}$. The correlator corresponding to the loss spectrum in Eq. (17) is given by the Mittag-Leffler function of index a: $M_a(x)=\Sigma_{n=0}^{\infty}x^n/\Gamma(1+na)$,

$$\phi_q(t) = f_q^c + \chi_{0q}^{cc} M_a[-(t\omega_q^c)^a]. \quad (18)$$

The Mittag-Leffler function can be calculated efficiently by Fourier-back transformation of $\chi_q''(\omega)/\omega$.

Equation (17) describes a very broad peak for the loss spectrum $\chi_q''(\omega)$ with a maximum located at $\omega=\omega_q^c$. The spectrum is invariant under the interchange of (ω/ω_q^c) to (ω_q^c/ω): the $\chi_q''(\omega)$-versus-log ω curve is symmetric. The width of the peak increases strongly with decreasing exponent a. For $a\approx 0.3$, ω must increase by more than a factor of 10^4 in order to scan the interval of frequency where $\chi_q''(\omega) \geqslant \chi_q''(\omega_q^c)/2$. This susceptibility formula known as Cole-Cole law, Eq. (17), was introduced as an empirical formula for dielectric loss spectra in glassy systems [13]. In particular, broad peaks located above the α peaks—often called β-peaks in this context—have been fitted by it.

The Cole-Cole formula, Eq. (17), exhibits simple limits for small and large frequencies. For $(\omega/\omega_q^c)^a \ll 1$, the Cole-Cole susceptibility reproduces the general power law for the loss spectrum, Eq. (11c), $\chi_q''(\omega) \propto \omega^a$. Similarly, the corresponding Mittag-Leffler correlator reproduces the general long-time asymptote for the response, Eq. (10). For $(\omega/\omega_q^c)^a \gg 1$, the Cole-Cole spectrum describes a critical spectrum which decreases with increasing frequency, $\chi_q''(\omega) \propto 1/\omega^a$. This is similar to a von Schweidler law spectrum. The corresponding Mittag-Leffler correlator decreases according to the law $\phi(t)-\text{const} \propto -t^a$. This yields a response function $\chi(t) \propto 1/t^x$ with $x=1-a<1$. Such behavior is consistent with the one detected by the OKE results for van der Waals liquids [9].

The crossover of the critical spectrum from the low-frequency wing to the high-frequency wing of the Cole-Cole loss peak has a counterpart for the Mittag-Leffler correlator that is most easily seen in a semilogarithmic plot. For $(t\omega_q^c)^a \ll 1$, the $[\phi(t)-\text{const}]$-versus-log t curve is bent downward, as known for the von Schweidler curves. For $(t\omega_q^c)^a \gg 1$, there is the critical power-law decay which shows up as an upward-bent curve. Hence, the $\phi(t)$-versus-log t curve exhibits an inflection point. For an exponent a around 0.3, the curve is nearly straight for an increase of $\log_{10} t$ by a factor of about 3. In this case, there is nearly logarithmic decay of the critical correlator for a time variation over three orders of magnitude.

It depends on the size of $1/\omega_q^c$ relative to the microscopic time scale t_{mic} which part of the Mittag-Leffler correlator dominates the critical dynamics in the time range of interest. The crucial question concerns the range of validity of the leading-order result for the susceptibility and for the modulus. These ranges are determined by the correction amplitudes. If $|\hat{K}_q|$ is large and $|\hat{K}_q^m|$ small, the Cole-Cole formula has a larger range of applicability than the general simple power-law formula (11c). But, if $|\hat{K}_q^m|$ is larger than $|\hat{K}_q|$, Eq. (11c) is a better approximation for the critical decay than the Cole-Cole spectrum. Since the square brackets in Eqs. (13) are positive, there are two obvious results. If $\hat{K}_q$ is positive, there holds $\hat{K}_q^m > \hat{K}_q$. In this case, the leading-order result for the susceptibility is a better description of the critical spectrum than the Cole-Cole spectrum. If $\hat{K}_q^m$ is negative, there holds $|\hat{K}_q^m| < |\hat{K}_q|$ and the application of the Cole-Cole law is superior to the one of the general leading-order result for the loss spectrum. For negative correction amplitudes $\hat{K}_q$, there is a trend for cancellation of the two contributions to $\hat{K}_q^m$ in Eq. (13c). It is a generic situation, that $|\hat{K}_q^m|$ is smaller than $|\hat{K}_q|$. Hence, for $\hat{K}_q<0$, it is expected that the Cole-Cole law is a good description of the critical dynamics.

A detailed discussion of the MCT equations has shown that a large arrested part f_q^c implies a large negative correction amplitude $\hat{K}_q$ for the critical decay [14]. In this case, the onset time t_q^* may exceed the microscopic time scale t_{mic} by several orders of magnitude. The time range for the applica-

bility of the leading-order asymptotic description of the critical decay may be outside the accessible range of the existing spectrometers. But, this is the situation, where $|\hat{K}_q^m|$ may be so small that the Cole-Cole law or the Mittag-Leffler correlator can provide an adequate description of the critical dynamics.

IV. APPLICATION TO SCHEMATIC MODELS

The preceding results shall be demonstrated in a simple schematic model for two different cases where the model parameters are adjusted to reproduce the data measured for benzophenone (BZP) and salol [9,10,12]

The simplest MCT models deal with a single correlation function only. For these models, the formulas in the preceding sections simplify since the label q can be dropped. The correlator, the critical arrested part, and the critical amplitude shall be denoted by $\phi(t)$, f^c, and h, respectively. The model is specified by the frequency Ω and the friction coefficient ν in the equation of motion (2a). Furthermore, there are the non-negative coefficients v_l, $l \geqslant 1$, which specify the mode-coupling monomial of order l for $\mathcal{F}$ in Eq. (2b). In applications for data descriptions, the specified numbers are considered as smooth functions of the physical control parameters.

The simplest model for the polynomial $\mathcal{F}$, which can reproduce all possible values for the exponent parameter λ, is given by the following formula for the fluctuating-force kernel:

$$m(t) = v_1 \phi(t) + v_2 \phi(t)^2. \tag{19}$$

The two coupling constants v_1 and v_2 specify the state of the system by a point in the first quadrant of the v_1-v_2 plane, cf. lower inset in Figs. 1 and 4. The points (v_1^c, v_2^c) for generic fold bifurcations are located on a piece of a parabola. The position of the specific transition point can be characterized by the value for λ [17]:

$$v_1^c = (2\lambda - 1)/\lambda^2, \quad v_2^c = 1/\lambda^2, \quad f^c = 1 - \lambda, \quad h = \lambda. \tag{20a}$$

The separation of some point (v_1, v_2) from the transition point (v_1^c, v_2^c), see upper insets Figs. 1 and 4, is given by

$$\sigma = [\hat{v}_1 + \hat{v}_2(1-\lambda)]\lambda(1-\lambda), \quad \hat{v}_{1,2} = v_{1,2} - v_{1,2}^c. \tag{20b}$$

The arrested part of the correlator for the glass state reads $\phi(t \to \infty) = h[\sigma/(1-\lambda)]^{1/2} + \mathcal{O}(\sigma^{3/2})$. The splitting of this value in an amplitude h and a remainder is not unique. The cited value for the critical amplitude h follows the conventions made in the preceding literature [14]. The general expression for the correction amplitude $\hat{K}$ for $M=1$ models [18] is specialized easily to $\hat{K} = \kappa(x)$, where the function $\kappa(x)$ is defined by

$$\kappa(x) = \tfrac{1}{2}\Gamma(1-x)^3/[\lambda\Gamma(1-3x) - \Gamma(1-x)\Gamma(1-2x)]. \tag{21}$$

Function $\kappa(x)$ increases monotonically with increasing λ: it decreases with increasing x. For $\lambda = 1/2$, i.e., for $a = 0.395\ldots$, one gets $\kappa(a) = -0.169\ldots$. For λ approaching 1, a tends to zero and $\kappa(a)$ diverges. For $a = 1/3$, $\lambda = 0.684\ldots$, the correction amplitude vanishes. All higher-order corrections for the critical decay outside the transient regime vanish as well for this special value of λ [19]. Therefore, for λ near 0.7, the simple power-law formulas of the leading-order asymptotic-expansion theory like Eqs. (8), (10), and (11c) describe the critical dynamics very well.

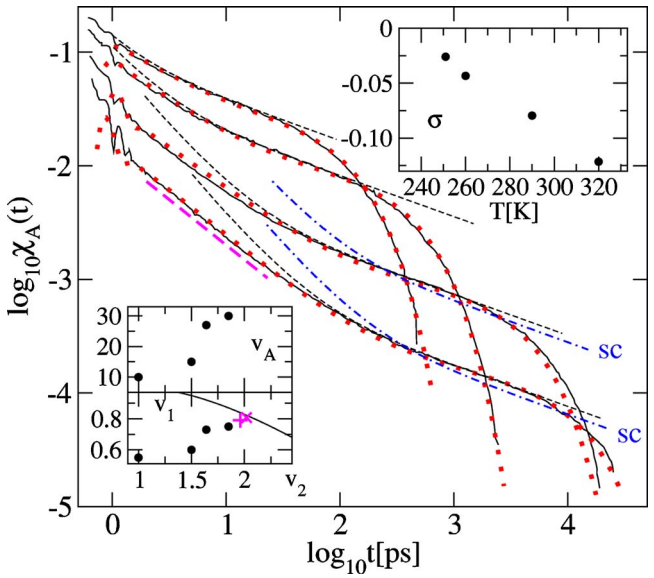

FIG. 1. (Color online) OKE response functions measured for BZP for $T/K = 251, 260, 290, 320$ [9] (full lines from bottom to top) and fits by the schematic-model functions $\chi_A(t)$ [12] (dotted lines). The straight dashed line has slope −0.80. The dashed-dotted lines labeled sc are the approximations by the scaling functions Eq. (28), the thin dashed lines are fits with Eq. (28) for freely adjusted s_σ and t_σ. The insets show the separation parameter σ (right) and the fitting parameters (left); two additional state points (+ and ×) indicate extrapolations for which solutions are shown in Fig. 7.

For the specified model, there holds $f^c \leqslant 1/2$. Hence, this model cannot be used to describe glassy-dynamics data for systems where the α-peak loss spectra have a weight f^c which exceeds 50% of the total weight. Moreover, the relation between the exponent parameter λ and the critical arrested part f^c, as formulated by Eq. (20a), is an artifact of the model. The minimum requirement for a schematic model for data analysis is the freedom to adjust λ and f^c independently. This goal can be achieved by introducing a second correlator. The first correlator $\phi_{q=1}(t) = \phi(t)$ is used as a caricature of the density-fluctuation dynamics. It provides the exponent parameter. The second one describes the dynamics of some probing variable, say, A. The correlator shall be denoted by $\phi_{q=2}(t) = \phi_A(t)$. All quantities referring to this correlator shall be indicated by an index A. The equation of motion (2a) is specified by $\Omega_A > 0$, $\nu_A \geqslant 0$, and a kernel $m_A(t)$. The two frequencies quantify the transient dynamics. The kernel is a polynomial (2b) of the two correlators involved. The simplest model describing the coupling of the probing variable to the density fluctuation is given by [20]

$$m_A(t) = v_A \phi(t) \phi_A(t). \tag{22}$$

The coupling of the probing variable to the density fluctuations is quantified by $v_A > 0$. Since there is no influence of the dynamics of the probing variable on the density dynamics, the same scaling law function $g_\pm(t/t_\sigma)$, Eq. (5a), describes the leading-order near-plateau dynamics of $\phi_A(t)$ as it does for that of $\phi(t)$. Notice in particular that the parameters Ω_A, ν_A, and v_A do not modify the time scale t_0. In applications for data descriptions, the model parameters Ω_A, ν_A, and v_A are to be considered as smooth functions of the physical control parameters, cf. lower insets in Figs. 1 and 4.

The loss spectrum $\chi''_A(\omega)$ develops a β peak upon increasing the mode-coupling coefficient v_A [21]. For this special case and in the limit of infinite v_A, the Cole-Cole susceptibility and the Mittag-Leffler correlator have been derived for the critical dynamics of the probing variable in Ref. [18]. The model specified by Eqs. (19) and (22) was used repeatedly for the description of experimental data [12,22–26]. Large data sets for the evolution of the glassy dynamics of propylene carbonate have been analyzed in Ref. [27]; results measured for different probing variables A obtained by neutron-scattering, depolarized-light-scattering, and dielectric-loss spectroscopy have been fitted by a common first correlator $\phi(t)$. The different probes have been characterized by adjusting the parameters for the second correlator $\phi_A(t)$ only.

Up to order $(t_0/t)^{2a}$, the kernel $m_A(t)$ can be calculated from Eq. (22) substituting the expression (9a) for $\phi(t)$ and the analog expression for the second correlator,

$$\phi_A(t) = f_A^c + h_a(t_0/t)^a[1 + \hat{K}_A(t_0/t)^a]. \tag{23}$$

Laplace transform yields $\omega m_A(\omega)$ as an asymptotic power series in the small parameter $\xi = (-i\omega t_0)^a$. The coefficients are linear functions of f_A^c, h_A, and $\hat{K}_A$. This is substituted on the left-hand side of Eq. (3a) for $q=2$. Expanding the right-hand side up to orders ξ^2, one can compare the coefficients in order to arrive at

$$f_A^c = 1 - [1/(f^c v_A)], \quad h_A = \lambda/(f^{c2} v_A). \tag{24}$$

The correction amplitude shall be noted in the convention of the general theory [14]:

$$\hat{K}_A = \kappa(a) + K_A, \tag{25a}$$

$$K_A = \lambda v_a \left(\frac{1}{v_A(1-\lambda)} - \lambda \right) \Big/ [v_A(1-\lambda) - 1]. \tag{25b}$$

This leads to the parameters for the Cole-Cole susceptibility:

$$\chi_{0A}^{cc} = 1/(f^c v_A), \quad \omega_A^c t_0 = \{(1-\lambda)/[\lambda\Gamma(1-a)]\}^{1/a}. \tag{26}$$

Remarkably, the comparison of Eq. (26) with the general expression in Eq. (16b) shows, that the Cole-Cole frequency ω_A^c does not depend on the coupling coefficient v_A. $\omega_A^c t_0$ decreases with increasing λ from 0.37…for $\lambda = 1/2$ to about 10^{-4} for λ near 0.88. For λ around 0.7, $\omega_A^c t_0$ is about 0.02.

A. Critical relaxation for a small Cole-Cole frequency

Figure 1 reproduces OKE-response functions measured for benzophenone (BZP) [9] and fits to these data by the response $\chi_A(t)$ calculated for the model defined in the preceding section. The fit parameters for the mode-coupling coefficients v_1, v_2, and v_A are specified in the lower inset. The analysis shall be done by anticipating a transition point for $\lambda = 0.70$, which implies the exponents $a = 0.33$ and $b = 0.64$. The cross in the inset is close to this bifurcation point. The σ-versus-T diagram is shown in the upper inset; and extrapolation to $\sigma = 0$ suggests the critical temperature $T_c = 235$ K with an estimated uncertainty of ± 5 K. The 251 K result exhibits the expected von Schweidler decay, $\log \chi(t) = \text{const} - (1-b)\log t$ for times between about 0.3 ns and about 6 ns. Further details can be inferred from Ref. [12].

The MCT results describe the measured evolution of the glassy dynamics adequately for times exceeding $t_{\text{mic}} = 1$ ps with two exceptions. The $T = 251$ K data exhibit a pronounced oscillation near 1.1 ps, while the calculated curve shows this oscillation near 0.9 ps. Furthermore, there are some deviations between the theoretical results and the data for the $T = 260$ K results for times around 10 ns. The four correlators $\phi_A(t)$ and the four loss spectra $\chi''_A(t)$, which are shown in the lower panels of Figs. 2 and 3, respectively, are the MCT results corresponding to the MCT responses $\chi_A(t)$ shown in Fig. 1. The data fits have been calculated for fixed relative values of the four frequencies, which specify the transient dynamics: $\Omega_A = \Omega$, $\nu_A = \nu = 5\Omega$. The scale Ω for the fits is chosen different for different temperatures T [12]. The curves in Figs. 2 and 3 are presented with a T-independent scale corresponding to that one used for the fit for $T = 251$ K: $\Omega = 1.67$ ps^{-1}. With the mentioned reservations, these curves can be considered as the measured quantities for the OKE-probing variable A. The full lines marked c in Figs. 2 and 3 show the critical correlator $\phi_A^c(t)$ and the critical loss spectrum $\chi''^c_A(\omega)$, respectively, for the transition point specified by $\lambda = 0.70$ and $v_A = 30$. The correlator relaxes to the plateau $f_A^c = 8/9$ with a critical amplitude $h_A = 7/27$.

The second scaling law for the decay below the plateau of the correlators, Eq. (7), implies a corresponding scaling law for the response

$$\chi_A(t) = \tilde{\chi}_A(t/t'_\sigma)/t'_\sigma. \tag{27}$$

The control-parameter independent shape function reads $\tilde{\chi}_A(\tilde{t}) = -\partial\tilde{\phi}_A(\tilde{t})/\partial\tilde{t}$. The reader can check this superposition principle for the results in Fig. 1 as follows. The $\log \chi_A(t)$-versus-$\log t$ curve for $T = 320$ K and $t \geqslant 2$ ps can be translated so that it collapses with the curves for $T/\text{K} = 290$, 260, and 251 for times exceeding 4 ps, 90 ps, and 290 ps, respectively. Equivalently, the four loss spectra in Fig. 3 for $\chi''_A(\omega) \geqslant 0.1$ are connected by the superposition principle, $\chi''_A(\omega) = \tilde{\chi}''_A(\omega t'_\sigma)$. The von Schweidler law describes a part of the high-frequency wing of the loss peak as shown by the straight dashed line with label vS for the $T = 251$ K curve. The Kohlrausch law for a stretching exponent $\beta = 0.91$ describes the upper part of the α peak as shown by the dashed line with label K for the $T = 260$ K result.

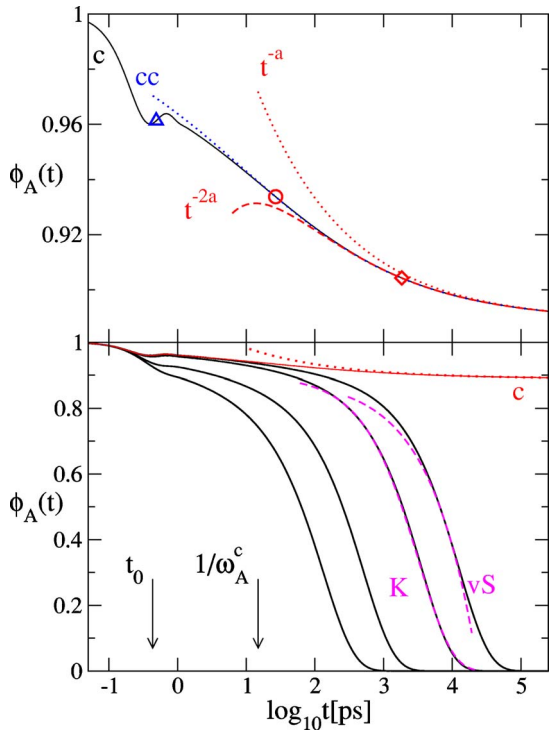

FIG. 2. (Color online) Correlation functions for BZP. The lower panel exhibits the correlators $\phi_A(t)$ underlying the fits in Fig. 1 (heavy full lines from left to right for $T/K=320$, 290, 260, and 251, respectively). The light full line with label c shows the critical correlator calculated for $\lambda=0.7$ and $v_A=30$. The dotted line is the leading asymptotic law, Eq. (8), with the time scale $t_0=0.3775$ ps. The dashed line marked vS shows a von Schweidler law, Eq. (6), with $b=0.64$ and a time scale adjusted to match the $T=251$ K curve. The dashed line labeled K is a fit by the Kohlrausch law, $\phi_A(t)=f_A^c \exp[-(t/\tau)^\beta]$, $\beta=0.91$, with τ adjusted to match the $T=260$ K curve. The times t_0 and $1/\omega_A^c=15$ ps are indicated by arrows. The upper panel shows the critical decay (c) together with the leading-order (t^{-a}) and next-to-leading-order (t^{-2a}) asymptotic power-law solution, Eq. (9a). The dotted curve labeled cc displays the leading-order Cole-Cole solution, Eq. (18), with $\chi_0^{cc}=1/9$. The points of 10% deviation of the approximations t^{-a}, t^{-2a}, and cc from the critical decay are indicated by the diamond, circle, and triangle, respectively.

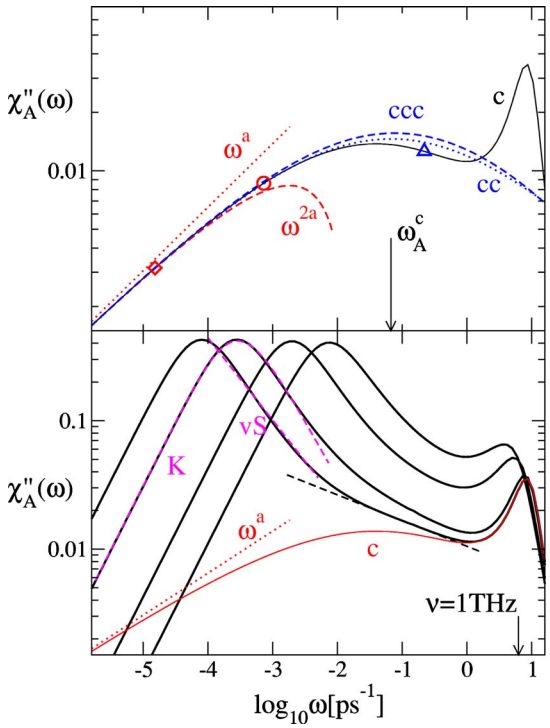

FIG. 3. (Color online) Spectra for BZP. The lower panel shows the susceptibility spectra for the correlators from the lower panel of Fig. 2. The leading-order critical spectrum, Eq. (11c), is the dotted straight line marked by ω^a. A dashed straight line with slope −0.2 is fitted to the $T=251$ K spectrum to indicate an $\omega^{-b'}$ law for $b'=-0.2$. In the upper panel, the dashed curve marked ω^{2a} shows the approximation by Eq. (11a). The approximation by the Cole-Cole function (cc), Eq. (17), is shown dotted, the inclusion of the correction, Eq. (15) yields the dashed curve labeled ccc for $\omega_A^c=67$ ns^{-1}. The points of 10% deviation of the approximations ω^{-a}, ω^{-2a}, and cc from the critical spectrum are indicated by the diamond, circle, and triangle, respectively. The frequencies ω_A^c and $\nu=\omega/(2\pi)=1$ THz are marked by arrows.

There is an interval of times between the end of the transient dynamics and the start of the von Schweidler decays that deals with the relaxation towards and through the plateau f_A^c. The dynamics causes the loss spectra for $\chi_A''(\omega)\leqslant 0.1$ and $\omega/(2\pi)<0.1$ THz shown in Fig. 3. The leading order asymptotic solution of the MCT equations of motion deals with this part of the dynamics together with the von Schweidler law part by Eq. (5a). This formula yields the first scaling law for the response

$$\chi_A(t) = h_A s_\sigma \hat{\chi}(t/t_\sigma), \quad s_\sigma = \sqrt{|\sigma|}/t_\sigma. \tag{28}$$

The shape function reads $\hat{\chi}(\hat{t})=-\partial g_\pm(\hat{t})/\partial\hat{t}$, $T\gtrless T_c$. For $T>T_c$, Eq. (4b) yields the von Schweidler response for large rescaled times $\hat{t}=t/t_\sigma$: $\hat{\chi}(\hat{t}\gg 1)=B\cdot b/\hat{t}^x$, $x=1-b<1$. For small rescaled times, Eq. (4a) yields $\hat{\chi}(\hat{t}\ll 1)=a/\hat{t}^x$, $x=1+a>1$. The crossover from one asymptote to the other occurs for times near t_σ. The light dashed lines in Fig. 1 exhibit fits of the data by Eq. (28) for $\lambda=0.70$. However, both scales s_σ and t_σ are adjusted with the aim to achieve a good match in the von Schweidler law regime. The $1/t^{1+a}$ law is not exhibited by the results in Fig. 1. For $T=320$ K, the crossover time t_σ is located near 1 ps, i.e., it is within or close to the transient regime. For the other three temperatures and times within the interval $t_{\rm mic}<t<t_\sigma$, the measured response and the calculated functions $\chi_A(t)$ are below the values of $h_A s_\sigma \hat{\chi}(t/t_\sigma)$.

The straight dashed line in Fig. 1 has a slope of −0.80. It demonstrates a pseudo-von Schweidler decay of the $T=251$ K results for 2 ps$<t<$20 ps: $\phi_A(t)-\text{const}\propto -t^{b'}$, $b'=0.20$. The $\phi_A(t)$-versus-log t curves in Fig. 2 for $t>2$ ps approach and cross the plateau as downward-bent curves before entering the von Schweidler decay regime. There are no inflection points of the curves for some time near t_σ, as implied by Eq. (5a).

The first scaling law describes a loss minimum of some value $\chi_{\rm min}$ at some position $\omega_{\rm min}$. The shape of the

log $\chi''_A(\omega)$-versus-log ω curves is independent of the separation parameter σ and the scales fix the position of the curve, $\chi_{\min} \propto \sqrt{|\sigma|}$, $\omega_{\min} \propto 1/t_\sigma$. The minimum is due to the crossover from the von Schweidler wing of the α peak, $\chi''(\omega) \propto 1/\omega^b$, to the power-law asymptote for the critical dynamics, $\chi''(\omega) \propto \omega^a$. For most practical purposes, the minimum can be approximated by the interpolation formula [28]:

$$\chi''_A(\omega)/\chi_{\min} = [b(\omega/\omega_{\min})^a + a(\omega_{\min}/\omega)^b]/(a+b). \quad (29)$$

However, the loss spectra in the lower panel of Fig. 3 do not exhibit loss minima, which can be described by the interpolation formula for the leading-order asymptotic result. The minima for frequencies ω near 1 ps^{-1} do not depend sensitively on σ. With decreasing $|\sigma|$, the minimum position even shifts slightly upwards rather than downwards. With increasing frequency, the high-frequency part of the α peak exhibits a crossover from the von Schweidler decay, $\chi''(\omega) \propto 1/\omega^b$, to a pseudo-von Schweidler decay, $\chi''(\omega) \propto 1/\omega^{b'}$. For $T=251$ K, this high-frequency wing extends from $\omega \approx 0.02$ ps^{-1} to about 0.4 ps^{-1} with $b'=0.2$, as is demonstrated by the dashed straight line. The observed minimum is due to the crossover from the $1/\omega^{b'}$ wing to the spectral peak for the normal-liquid dynamics. The latter is located near $\nu=1$ THz.

The scaling law fits, which are shown in Fig. 1 by the light dashed lines, are misleading because the scales s_σ and t_σ have been adjusted freely. Calculating these scales from Eqs. (5b), (20b), and (24), one obtains for $T=251$ K and 260 K the dashed-dotted lines marked by sc. The two distance parameters $\varepsilon=(T_c-T)/T_c$ are −0.07 and −0.11, respectively. These values are too large for a leading-order asymptotic formula to be applicable.

The correlator $\phi_A(t)$ for the lowest temperature under discussion is close to the critical one for t up to about 30 ps, as is shown in the lower panel of Fig. 2. Hence, the $T=251$ K curves exhibit critical glassy dynamics for the times between 1 ps and 30 ps. From Eqs. (25) one obtains the correction amplitude $\hat{K}_A=-1.51$. This large value yields an onset time t_A^* for the t^{-a} law which is beyond $t=10^3$ ps as is marked by the diamond in the upper panel of the figure. Including the leading correction term yields the approximation by the dashed line denoted t^{-2a}. It improves the description of the critical decay so that it can be understood for times larger than about $t=30$ ps. But the expansion formula (23) cannot be used to describe that part of the critical decay, which is measured for BZP and described by the solution of the two-component schematic MCT model.

Substituting the cited values for λ, f_A^c, and h_A into Eqs. (13a) and (13b), one gets the plateau for the modulus, $f_A^{mc}=8$, and the critical amplitude $h_A^m=21$. Notice that the relative strength of the first scaling law amplitude for the modulus is much larger than that for the correlator, $h_A^m/f_A^{mc}=2.6$ versus $h_A/f_A^c=0.29$. From Eq. (13c), one obtains the correction amplitude $\hat{K}_A^m=0.124$. As expected from the discussions of Sec. III, the onset time t_A^{m*} for the leading order formula for the modulus,

$$m_A(t) = f_A^{mc} + h_A(t_0/t)^a, \quad (30a)$$

is smaller than t_A^* by more than a factor 1000. As a result, see the upper panel of Fig. 2, the equivalent formula (18) for the correlator,

$$\phi_A(t) = f_A^c + (1-f_A^c)\mathbf{M}_a[-(t\omega_A^c)^a], \quad (30b)$$

describes the probing variable A for all times exceeding $t=1$ ps. The leading-order asymptotic result for the modulus explains the response for $T=251$ K quantitatively within the interval 1 ps $\leqslant t \leqslant 30$ ps.

Figure 3 shows that the leading asymptotic description of the critical loss spectrum, Eq. (11c), would be relevant for the explanation of the loss minimum only in cases with $\omega_{\min} < 2\times 10^{-5}$ ps^{-1}. The dashed line labeled ω^{2a} exhibits the asymptotic expansion for the critical loss up to the leading correction, Eq. (11a). This formula is relevant for $\omega < 10^{-3}$ ps^{-1}. Even this expression is unsatisfactory for the discussion of the BZP results because of the large correction amplitude. However, the Cole-Cole spectrum describes the critical loss reasonably for $\omega < 0.2$ ps^{-1}. The correction amplitude for the Cole-Cole law, Eq. (16c) is very small, $\hat{K}_A^{cc}=0.076$. The Cole-Cole law with leading correction, Eq. (15), is shown in the upper panel of Fig. 3 by the curve marked ccc, and is slightly above the leading-order result in the regime of large frequencies.

For the system under study, the Cole-Cole frequency reads $\omega_A^c=0.067$ ps^{-1}. This frequency $\omega_A^c/(2\pi) \approx 10$ GHz is small compared to the 1 THz scale for the normal-liquid dynamics. The value $-\log \omega_A^c$ is in the center of the $\log t$ interval studied by the results of Fig. 1. Therefore, the critical spectrum relevant for the understanding of the data differs qualitatively from the leading-order power-law formula. As a result, the loss minima in Fig. 3, which are caused by the superposition of the critical spectra for ω near and above ω_A^c and the von Schweidler law wing of the α peak, differ drastically from the general low-frequency shape described by Eq. (29). For $T=251$ K, the superposition yields the pseudo-von Schweidler law manifested as a wing specified by the exponent $b'=0.20$. This wing will be analyzed further in Sec. V.

B. Critical relaxation for an intermediate Cole-Cole frequency

Five OKE response functions measured for salol [10] and fits by the functions $\chi_A(t)$ of the above explained schematic model are reproduced in Fig. 4. The filled dots in the insets specify the mode-coupling coefficients v_1, v_2, and v_A used for the calculations. Further details can be found in Ref. [12], where, however, the value for Ω was misprinted. The series of states (v_1, v_2) extrapolates to a transition point with $\lambda=0.73$, which implies a critical exponent $a=0.31$ and a von Schweidler exponent $b=0.59$. The extrapolation of the σ-versus-T parameters to $\sigma=0$ suggests a critical temperature $T_c=245$ K with an estimated uncertainty of ±3 K. The MCT correlators $\phi_A(t)$ and loss spectra $\chi''_A(\omega)$, which are equivalent to the response $\chi_A(t)$ in Fig. 4, are shown in the lower panels of Figs. 5 and 6, respectively. They can be considered as the measured results for the glassy dynamics

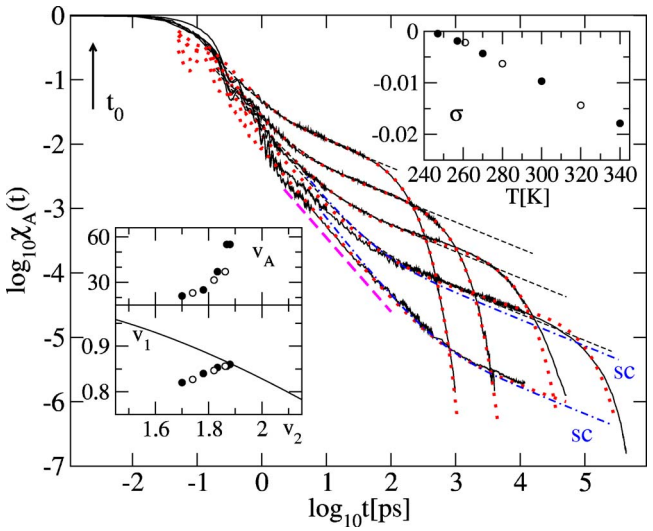

FIG. 4. (Color online) OKE-response functions measured for salol for $T/\mathrm{K}=247$, 257, 270, 300, 340 (full lines from bottom to top) [10]. The dotted lines are fits by the schematic-model response $\chi_A(t)$ calculated with $\Omega=2\Omega_A=10\nu_A=15.9\ \mathrm{ps}^{-1}$ [12]. Symbols and curve styles are the same as in Fig. 1. The slope of the straight dashed line is −1.15.

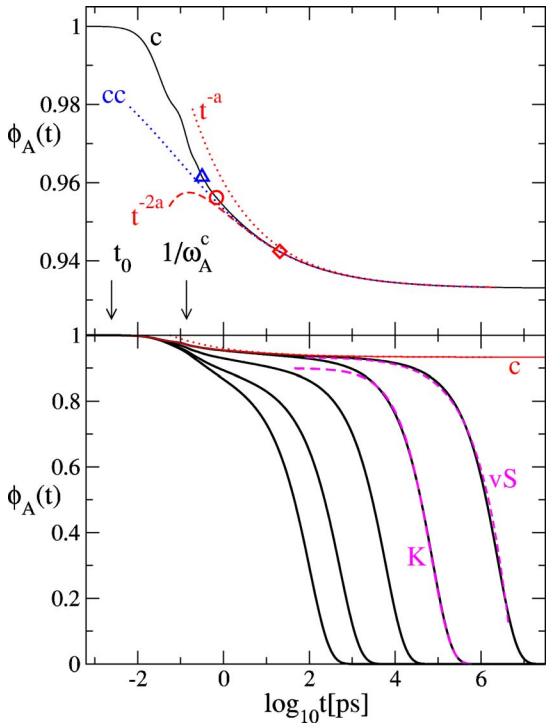

FIG. 5. (Color online) Correlation functions for salol. The lower panel shows the correlators $\phi_A(t)$ used for the response fits in Fig. 4 for $T/\mathrm{K}=247$, 257, 270, 300, and 340 (heavy full lines from right to left). The light full line shows the critical correlator calculated for $\lambda=0.73$, and $v_A=55$. The dashed line marked vS exhibits a von Schweidler law, Eq. (6), for a time scale chosen to match the $T=247$ K correlator. The dashed line marked K is a Kohlrausch-law fit for the $T=257$ K curve with exponent $\beta=0.95$. The dotted line exhibits the formula (8) with $t_0=0.002\,46$ ps. The upper panel shows the critical decay (c) together with the leading- (t^{-a}) and next-to-leading-order asymptotic solution (9a) (t^{-2a}). The dotted curve labeled cc displays the leading-order solution from Eq. (18) with $\chi_0^{cc}=0.067$ and $\omega_A^c=7.25$ ps. The points of 10% deviation of the approximations t^{-a}, t^{-2a}, and cc from the critical decay are indicated by the diamond, circle, and triangle, respectively. The times t_0 and $1/\omega_A^c$ are marked by arrows.

of salol, since the calculated and measured curves in Fig. 4 agree outside the transient regime. This holds with the reservation, that fits and measurements for the $T=270$ K results exhibit some discrepancies for times exceeding 20 ns. The lines with label c in Figs. 5 and 6 show critical correlators and critical loss spectra, respectively, calculated for $\lambda=0.73$ and $v_A=55$. The correlators relax to the plateau $f_A^c=0.93$ with a critical amplitude $h_A=0.18$.

The test of the superposition laws for the long-time relaxation parts of the correlators is left to the reader. This second scaling law of MCT relates the α-relaxation peaks for the loss spectra for $\chi_A''(\omega)\geqslant 0.1$. Kohlrausch-law fits and von Schweidler asymptotes have been added to the data for $T=257$ K and $T=247$ K, respectively, in order to emphasize that the results for the evolution of the below-plateau-decay process follows the familiar pattern. Notice that the response for $T=257$ K exhibits the von Schweidler law decay, $\log\chi_A(t)=\mathrm{const}-(1-b)\log t$ for the large time interval 0.1 ns $\leqslant t\leqslant 10$ ns. The measurement for this temperature permits a rather precise determination of the exponent b and, thereby, of λ.

The light-dashed lines in Fig. 4 are fits of the data by the first-scaling-law expression (28) with freely adjusted scales s_σ and t_σ. For $T\geqslant 270$ K, these fits describe the data outside the transient regime up to times within the von Schweidler law region. A more detailed documentation of this result can be found in Ref. [10], where also consistency of the fitted scales s_σ, t_σ, and t_σ' with the MCT-power-law formulas was demonstrated. The scaling-law results calculated with the MCT values for the scales h_A, s_σ, and t_σ in Eq. (28) are shown in Fig. 4 as dashed-dotted lines marked sc for the $T=257$ K and $T=247$ K data. For $T=257$ K, $\varepsilon=-0.05$ is so large, that Eq. (28) cannot account quantitatively for the scales ruling the von Schweidler law decay. For $T\geqslant 270$ K the distance parameter ε exceeds 10%; the leading asymptotic expansion formula for the plateau-crossing process is not applicable for such large distances of the control parameter from the critical value. In contrast, the scaling law (28) describes the $T=247$ K result well for the large time interval 0.04 ns $<t<10$ ns. In this case, the distance parameter $\varepsilon=-0.008$ is so small that the leading-order expansion result for the plateau crossing, Eq. (5a), accounts for a major part of the long-time response—readjusting the scales ($h_A s_\sigma$), and t_σ would not improve the fit.

Figure 5 shows that the $T=247$ K response is close to the critical one for $t\leqslant 1$ ns. The straight dashed line with slope −1.15, which is shown in Fig. 4, demonstrates that the critical response exhibits a power-law decay $\chi_A(t)\propto 1/t^{1+a'}$, $a'=0.15$, for 2 ps $<t<100$ ps. This is equivalent to a power-law decay of the correlator, $\phi_A(t)-f_a^c\propto 1/t^{a'}$. In qualitative agreement with the prediction by Eq. (5a), the crossover from the t^{-a} decay to the $-t^b$ decay causes an inflection point for the $\phi_A(t)$-versus-log t curve in Fig. 5. The corresponding

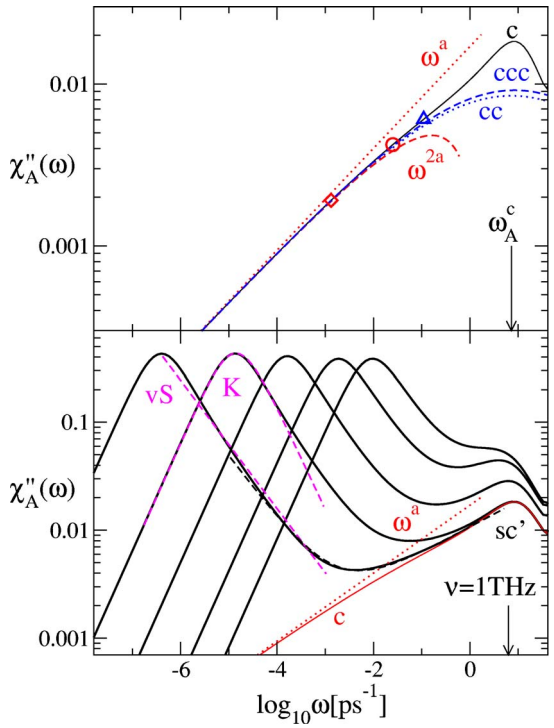

FIG. 6. (Color online) Spectra for salol. The lower panel shows the susceptibility spectra $\chi''_A(\omega)$ for the correlators shown in the lower panel of Fig. 5. The leading-order approximation to the critical spectrum, Eq. (11a), is shown as dotted straight line marked ω^a. The dashed line labeled sc′ exhibits the interpolation formula (29) with the von Schweidler exponent $b=0.59$ and the critical exponent a replaced by $a''=0.24$. The upper panel exhibits the critical spectrum as full line with label c, the leading-order asymptotic approximation, Eq. (11c), (dotted, labeled ω^a) and Eq. (11a), (dashed, labeled ω^{2a}). The approximation by the Cole-Cole function for $\omega^c_A=7.25\ \mathrm{ps}^{-1}$ (cc), Eq. (17), is shown dotted, the inclusion of the correction, Eq. (15), yields the dashed curve labeled ccc. The points of 10% deviation of the approximations ω^{-a}, ω^{-2a}, and cc from the critical spectrum are indicated by the diamond, circle, and triangle, respectively. The frequencies ω^c_A and $\omega/(2\pi)=\nu=1$ THz are marked by arrows.

crossover from the ω^{-b} wing of the α peak to some $\omega^{a''}$ spectrum causes the loss minimum located near $\log\omega=-2.5$ in Fig. 6. The dashed curve marked sc′ exhibits a description of this minimum by the function $\chi''_A(\omega)/\chi_{\min}=[b(\omega/\omega_{\min})^{a''}+a''(\omega_{\min}/\omega)^b]/(a''+b)$ which is suggested by Eq. (29). For salol, as opposed to BZP, the minimum position decreases strongly with decreasing $|\varepsilon|$, in qualitative agreement with the first scaling law results.

The inconsistent exponents for $T=247$ K in the regime $2\ \mathrm{ps}<t<100$ ps indicate that the leading-order asymptotic description is still not applicable; the exponents $a'=0.15$ obtained from the fit of the OKE data and $a''=0.24$ obtained from the fit of the corresponding minimum are different and both are smaller than the correct value of $a=0.31$. The deviation of the critical correlator from the leading-order power-law result (8) and (10) within the specified time interval is caused by the large value for the correction amplitude, $\hat{K}_A=-1.78$. This value implies an onset time for the t^{-a} decay of beyond 20 ps as shown by the diamond in Fig. 5. The high-frequency part of the loss minimum is located in the region $10\ \mathrm{ns}^{-1}<\omega<1\ \mathrm{ps}^{-1}$. Figure 6 demonstrates that the ω^a law does not describe the critical loss there. Inclusion of the leading correction terms for the analytic description of the critical dynamics, i.e., using Eq. (9a) for the correlator and Eq. (11a) for the loss spectrum, explains the result for $t\geqslant 0.6$ ps and $\omega\leqslant 25\ \mathrm{ns}^{-1}$, as demonstrated in Figs. 5 and 6, respectively.

From Eq. (13c), one derives the correction amplitude for the modulus $\hat{K}^m_A=0.177$. The leading-order formula (30a) for the relaxation kernel describes the kernel m_A outside the transient regime. The corresponding expression (30b) for the correlator and the equivalent Cole-Cole formula for the loss spectrum account for the critical glassy dynamics, as shown in Figs. 5 and 6. The Cole-Cole formula with correction term of amplitude $\hat{K}^{cc}_A=0.09$ yields a slight improvement compared to the equation based on $\hat{K}^{cc}_A=0$, as shown in Fig. 6 by the curve with label ccc. Equation (16b) leads to the Cole-Cole frequency for salol, $\omega^c_A=7.25\ \mathrm{ps}^{-1}$. This value is close to the loss peak for the normal-liquid dynamics: $\omega^c_A t_{\mathrm{mic}}\approx 1$. The part of the glassy critical loss spectrum which is relevant for the explanation of the data in Fig. 4 deals with the regime $10^{-4}\leqslant\omega/\omega^c_A\leqslant 10^{-1}$. Within this frequency interval, the Cole-Cole spectrum increases smoothly with ω. Therefore, the leading-order formulas (10) or (11c) describe the dynamics qualitatively. However, the true critical spectrum differs from its low-frequency asymptote, Eq. (11c). Hence, the description of the dynamics by the scaling law is not correct quantitatively. Within the specified interval, the $\log\chi''_A(\omega)$-versus-$\log\omega$ spectrum can be approximated reasonably by a straight line, $\log\chi''_A(\omega)\approx\mathrm{const}+a''\log\omega$, $a''=0.24$. As a result, the critical dynamics is approximated well by a power-law decay specified by an exponent a'' smaller than the critical exponent a.

In the preceding section, the critical spectra have been discussed for both small and intermediate Cole-Cole frequencies ω^c_q; the case of a large Cole-Cole frequency is found in the depolarized light-scattering spectra for CKN [3,29]. In the fits with a schematic model by Alba-Simionesco and co-workers [30,31] one can identify a Cole-Cole peak for the critical spectra, but the description with the power-law solution is superior if terms up to order ω^{2a} are considered.

V. COLE-COLE WING

Figures 1–6 demonstrate the scenarios for the evolution of the glassy dynamics for $\omega^c_q\ll t^{-1}_{\mathrm{mic}}$ and $\omega^c_q\approx t^{-1}_{\mathrm{mic}}$, respectively, for the probing variable described by the second correlator of a two-component schematic MCT model. Solutions for this model, which exemplify a scenario as shown in Fig. 3, have been discussed before by Cummins [32]. He pointed out that the evolution of the wing phenomenon obtained from the model is similar to the one known for dielectric-loss spectroscopy for glycerol and several van der Waals liquids [33]. He emphasizes also that the cited measurements refer to temperatures T below T_c, while the calculations are done for

$T > T_c$. Furthermore, the experimental data demonstrate the wing only for frequencies below 10 GHz $\approx 10^{-2} t_{\mathrm{mic}}^{-1}$. So far, no wing has been reported which occurs in the two-decade frequency window adjacent to the microscopic excitation region.

In order to describe the wing phenomenon quantitatively, one can extend the Cole-Cole formula so that the spectrum can be described also for small but nonvanishing separation parameters $\sigma = C\varepsilon \propto (T_c - T)/T_c$. The leading-order expression for the plateau-crossing process of the fluctuating force correlators reads in analogy to Eq. (5a): $m_q(t) = f_q^{mc} + h_q^m g_\pm(t/t_\sigma)$, $\varepsilon \gtrless 0$. Laplace transformation yields $\omega m_q(\omega) = -f_q^{mc} + h_q^m C(\omega)$. Function $C(\omega)$ obeys a scaling law,

$$C(\omega) = \sqrt{|\sigma|}\, c_\pm(\omega t_\sigma), \quad \varepsilon \gtrless 0, \tag{31}$$

with the control-parameter independent shape functions $c_\pm(\hat{\omega})$ given by the Laplace transforms $g_\pm(\hat{\omega})$ of the shape functions $g_\pm(\hat{t})$: $c_\pm(\hat{\omega}) = \hat{\omega} g_\pm(\hat{\omega})$. Substitution of $\omega m_q(\omega)$ into Eq. (3b) yields the desired result. Expansion of the right-hand side in terms of the small parameter $C(\omega)$ and comparison with the result for $\chi_q(\omega)$ following from Eq. (5a) reproduces the relations (13a) and (13b) for the critical arrested parts and critical amplitudes. One gets

$$\chi_q(\omega) = (1 - f_q^c)/\{1 - [h_q/(1 - f_q^c)]C(\omega)\}. \tag{32a}$$

Equation (32a) was found for the schematic model in Ref. [18] for the special case of the second correlator $\phi_A(t)$ and in the limit of infinite coupling strength v_A. It is shown here, that Eq. (32a) can be derived without such restrictions. The leading correction to Eq. (32a) can be calculated from the asymptotic expansions in Refs. [14,16] in a straightforward manner; however, the evaluation of the result for fitting data is rather involved. Focusing on the critical decay, one can extend the preceding formula by adding the large-frequency part of the correction:

$$\chi_q(\omega) = (1 - f_q^c)/\{1 - [h_q/(1 - f_q^c)]C(\omega) + \hat{K}_q^{cc}(-i\omega/\omega_q^c)^{2a}\}. \tag{32b}$$

This expression describes the small-ε dynamics for $\omega t_{\mathrm{mic}} < 1$ and frequencies extending down to the beginning of the von Schweidler law decay.

BZP exemplifies the case of such a small $\hat{K}_q^{cc}$ that the leading-order result for the modulus, Eq. (32a), can be used. Figure 7 demonstrates that this result accounts for the $T = 251$ K spectrum for the large dynamical range 10^{-3} ps$^{-1} < \omega < 1$ ps^{-1}. The scaling law result for the loss spectrum, $\chi_A''(\omega) = h_A C_A''(\omega)$, is shown as dotted line sc; it can describe only a part of the von Schweidler law spectrum for $\omega < 10^{-3}$ ps^{-1}, but is inadequate for larger frequencies. This observation for the dynamics in the frequency domain is equivalent to the one demonstrated in Fig. 1 for the results in the time domain. The second scaling law result for the loss spectrum is exhibited as dashed-dotted line. It follows from Eq. (7), $\chi_A''(\omega) = (\omega t_\sigma')\tilde{\phi}_A''(\omega t_\sigma')$, and accounts for the loss peak for $\omega < 10^{-3}$ ps^{-1}. Combining the result for the second scaling law for the modulus with the result for the first scaling law for the loss spectrum explains the BZP spectrum for

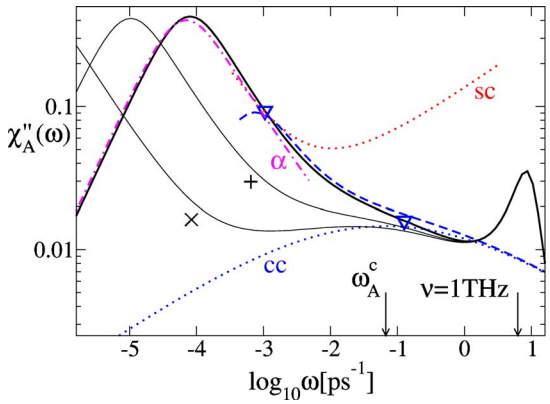

FIG. 7. (Color online) Asymptotic description of the wing in BZP. The heavy full line reproduces the BZP loss spectrum for $T = 251$ K from Fig. 3 and the dashed one exhibits the spectrum of the extended Cole-Cole susceptibility, Eq. (32a). The triangles mark the points of 10% deviation between these spectra. The dotted line sc is the first scaling law result for the susceptibility, and the line cc shows the Cole-Cole spectrum for the critical point. The dashed-dotted line represents the second scaling law result for the loss peak. The thin full lines are solutions corresponding to the state points indicated by + and × in Fig. 1.

$T = 251$ K for $\omega < 1$ ps^{-1} including in particular the α-peak wing. The small but systematic discrepancies between the loss spectrum in the structural-relaxation regime and the asymptotic MCT expressions result from the fact that the distance parameter $\varepsilon = (T - T_c)/T_c \approx 0.07$ is so large, that the asymptotic results for the scales still have noticeable errors while the shape functions already agree well with the nontrivial spectra.

Starting from the state that fits the 251 K data for BZP, a number of extrapolations are possible within the schematic model. Keeping all parameters but (v_1, v_2) fixed, two additional states shall be considered; they are indicated by × and + in the left-hand inset of Fig. 1; and their spectra are marked accordingly in Fig. 7. The first state point (×) is close to the transition point and is characterized by $\sigma = -0.003$ ($\varepsilon = -0.01$). Solutions at this point are shown in Ref. [12] for $\chi(t)$ and $\chi_A(t)$. The respective spectrum $\chi_A''(\omega)$ in Fig. 7 exhibits nearly constant loss for 0.4×10^{-3} ps^{-1} $< \omega < 0.4$ ps^{-1} within a 10% margin. In this frequency window the maximum around ω_A^c indicates an emerging Cole-Cole peak; the minimum at $\omega = 10^{-3}$ ps^{-1} is caused by the crossover of the high-frequency wing of the α peak and the low-frequency wing of the Cole-Cole peak. This minimum is ruled by the first scaling law and the divergent time scale t_σ. The second state (+) is an interpolation between × and the solution for BZP; the separation parameter is $\sigma = -0.01$ ($\varepsilon = -0.03$), and the point is chosen similar to the ones used in Fig. 4 of Ref. [32]. The spectrum in Fig. 7 shows a wing, $\chi_A''(\omega) \propto \omega^{-0.1}$, for almost three orders of magnitude in frequency. Hence, the crossover between α and Cole-Cole peaks can be interpreted as a power-law wing $\omega^{-b'}$ for some range in frequencies and control parameters without finetuning. The evolution of the crossover progresses from a wing with gradually lower exponents b' to nearly constant loss

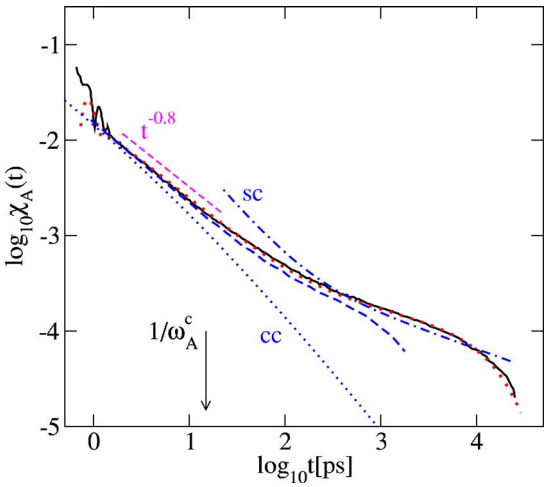

FIG. 8. (Color online) Asymptotic description of the OKE data for BZP. The full line reproduces the BZP data for $T=251$ K from Ref. [9]; the dotted line reproduces the fit from Fig. 1. The dashed curve, the dashed-dotted curve sc, and the dotted curve cc, respectively, show the Fourier backtransforms of the extended Cole-Cole susceptibility in Eq. (32a), of the first scaling law, and of the Cole-Cole law in Eq. (17), cf. Fig. 7.

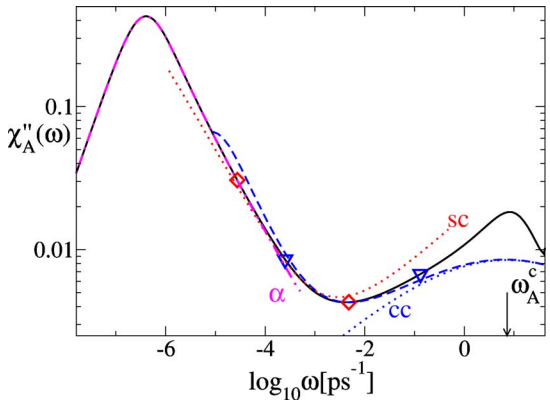

FIG. 9. (Color online) Asymptotic description of the minimum in salol. The full line reproduces the salol loss spectrum for $T=247$ K from Fig. 6 and the dashed one exhibits the spectrum of the extended Cole-Cole susceptibility, Eq. (32a). The triangles mark the points of 10% deviation between these spectra. The dotted line cc is the Cole-Cole spectrum for the critical point, and the line sc shows the first scaling law result for the susceptibility; the diamonds mark the points where sc deviates by 10% from the loss spectrum. The dashed-dotted line represents the second scaling law result for the loss peak.

and eventually the emergence of a Cole-Cole peak. While the extrapolations presented in this paragraph are not at all implied by the fit of the data, the scenarios seem nevertheless possible for realistic parameter values.

To conclude the discussion of BZP, let us return to the OKE data for $T=251$ K as shown in Fig. 8. In addition to data and fit for this state, the Fourier backtransforms of the asymptotic curves from Fig. 7 are displayed. While the asymptotic solution at the critical point (labeled cc) covers only less than a decade, the extended Cole-Cole susceptibility in Eq. (32a) describes the data over three orders of magnitude in time and thereby explains the $t^{-0.8}$ law found empirically. The remaining discrepancies are again due to the relatively large distance parameter for this state; Fig. 3 of Ref. [12] shows prefect agreement with the Cole-Cole law for states closer to the transition including state × from Fig. 1.

Different from the case for BZP, the lowest temperature available for salol, $T=247$ K, is described by a much smaller distance parameter, $\varepsilon \approx 0.01$, and therefore shares a larger frequency regime, say $\omega \lesssim 0.1$ ps^{-1}, with the critical loss spectrum, see the lower panel of Fig. 6. Being so close to the critical point, the second scaling law in Fig. 9—labeled α—is indistinguishable from the loss spectrum for $\omega \leqslant 10^{-4}$ ps^{-1}. The first scaling law sc describes the solution up to around $\omega \lesssim 0.005$ ps^{-1} which is the same as for the solution at the critical point, cf. upper panel of Fig. 6. As for the critical spectrum, the leading-order approximation in Eq. (32a) improves the description to larger frequencies by two decades up to $\omega \approx 0.1$ ps^{-1} before crossing over to the Cole-Cole peak which in this case is hidden under the microscopic excitations.

VI. CONCLUSION

Within the regime of glassy dynamics, susceptibilities $\chi_q(\omega)$ and moduli $\omega m_q(\omega)$ are related by Eq. (3b); and at the critical point, susceptibilities and moduli are both described by the universal power law ω^a. The range of validity of this power law is given by amplitudes for the correction ω^{2a}—$\hat{K}_q$ for the susceptibilities and $\hat{K}_q^m$ for the moduli, which are related by Eq. (13c). For some parameter regions a large value of $|\hat{K}_q|$ can render the power-law expansion for the susceptibilities irrelevant, while the correction amplitude $|\hat{K}_q^m|$ is so small that the universal power-law can be used for the description of the modulus successfully. Typically, this occurs if $\hat{K}_q$ is large and negative, and this can be expected if the plateau value f_q^c is high, cf. Eq. (13c). In this case, the susceptibility can be described well by the expansion of its inverse, Eq. (15). For vanishing correction $\hat{K}_q^m = K_q^{cc} = 0$, formula, the susceptibility at the critical point is given by the Cole-Cole law (17), a formula first introduced in 1941 [13].

The Cole-Cole frequency ω_q^c in Eq. (17) introduces a characteristic scale for assorting the critical dynamics into three categories. (1) If ω_q^c is large compared to the scale t_{mic}^{-1} for the band of normal liquid excitations, the Cole-Cole susceptibility reduces to the leading-order scaling law formula which is implied by Eq. (5a). There is a control-parameter sensitive minimum as discussed for Eq. (29) that interpolates between the von Schweidler law tail of the α peak, $\chi_q''(\omega) \propto 1/\omega^b$, and the critical spectrum $\chi_q''(\omega) \propto \omega^a$, where a and b are related via the exponent parameter λ. As an example for such a scenario one can cite the molten salt CKN. While the leading-order result alone is not sufficient to describe the measured data quantitatively, the power-law expansion in Eq. (11a) yields a satisfactory description that is superior to the Cole-Cole solution [29]. (2) If ω_q^c is close to t_{mic}^{-1}, one encounters a scenario demonstrated in Fig. 9 for salol. There is a control-parameter sensitive loss minimum. It originates from the crossover between the von Schweidler law tail and

the critical spectrum; and the critical spectrum approaches the maximum of the underlying Cole-Cole peak. A description by Eq. (29) is possible only, if the exponent a is replaced by some effective one a'', which is smaller than a, cf. Fig. 6. (3) If ω_q^c is smaller than the microscopic time scale, say $\omega_q^c t_{\mathrm{mic}} \approx 0.05$, we obtain the scenario seen in Fig. 7 for benzophenone (BZP). In this case, the von Schweidler law part of the α peak, $\chi_q'' \propto 1/\omega^b$, crosses over to some flatter wing, $\chi_q'' \propto 1/\omega^{b'}$, $a < b' < b$. This wing is caused by approaching the Cole-Cole spectrum for frequencies around the maximum at ω_q^c. For yet higher frequencies, one encounters a crossover—from the high-frequency part of the Cole-Cole spectrum for structural relaxation to the spectrum due to normal-liquid excitations—producing a different kind of a minimum. The position of this minimum is control-parameter insensitive. For the understanding of this minimum, both the scaling law (28) and the interpolation formula (29) are irrelevant. On the other hand, as shown in Sec. V and especially in Fig. 7, it is possible to describe the wing rather accurately by the leading-order formula (32a). If the α peak is shifted to yet lower frequencies, the wing can give way to a separate Cole-Cole peak.

All figures in this work have been prepared with model parameters that reproduce the OKE-response functions of benzophenone (BZP) and salol. Hence, Fig. 7 implies that the BZP spectra for temperatures near 250 K, when measured by depolarized light-scattering in backward direction, should exhibit an α peak wing for frequencies ν between about 1 GHz and about 100 GHz. The crossover from the von Schweidler law wing to the wing induced by the Cole-Cole peak is expected to occur around 1 GHz. This crossover position depends sensitively on the temperature, because the von Schweidler law relaxation depends sensitively on T.

The Cole-Cole law with correction, Eq. (15), has been derived in its fully general microscopic version in Sec. III; only in Secs. IV and V the theory was specialized to schematic models. While for the schematic models a number of parameters can be fixed to describe experimental data, for microscopic models the static structure of the model system determines these parameters uniquely. A first example for Cole-Cole dynamics in a microscopic model has been discussed recently for the mean-squared displacement $\delta r^2(t)$ of the hard-sphere system [34]; including the Mittag-Leffler function for the critical relaxation allows for an analytic description of the mean-squared displacement for the full range of the dynamics similar to BZP in Fig. 7. In addition, the Cole-Cole dynamics was identified in the data measured by van Megen *et al.* [35] where Eq. (15) accounts for the data for an interval in time of three orders of magnitude adjacent to the transient dynamics. Hence, the results discussed above seem relevant for both molecular and colloidal glasses and can be expected to facilitate more detailed investigations.

ACKNOWLEDGMENTS

The author thanks W. Götze for repeated help during the preparation of this work. The author is also grateful to L. Berthier, H. Z. Cummins, P. Lunkenheimer, E. Rößler, and Th. Voigtmann for enlightening discussions. Support was provided by DFG Grant No. SP 714/3-1 and NSF Grants Nos. DMR0137119 and DMS0244492.

[1] W. Götze, J. Phys.: Condens. Matter **11**, A1 (1999).
[2] W. Knaak, F. Mezei, and B. Farago, Europhys. Lett. **7**, 529 (1988).
[3] G. Li, W. M. Du, X. K. Chen, H. Z. Cummins, and N. J. Tao, Phys. Rev. A **45**, 3867 (1992).
[4] W. van Megen and S. M. Underwood, Phys. Rev. E **47**, 248 (1993).
[5] J. Wiedersich, N. V. Surovtsev, and E. Rössler, J. Chem. Phys. **113**, 1143 (2000).
[6] R. Torre, P. Bartolini, and R. M. Pick, Phys. Rev. E **57**, 1912 (1998).
[7] R. Torre, P. Bartolini, M. Ricci, and R. M. Pick, Europhys. Lett. **52**, 324 (2000).
[8] M. Ricci, P. Bartolini, and R. Torre, Philos. Mag. B **82**, 541 (2002).
[9] H. Cang, V. N. Novikov, and M. D. Fayer, J. Chem. Phys. **118**, 2800 (2003).
[10] G. Hinze, D. D. Brace, S. D. Gottke, and M. D. Fayer, Phys. Rev. Lett. **84**, 2437 (2000); **84**, 4783(E) (2000); J. Chem. Phys. **113**, 3723 (2000).
[11] L. Berthier and J. P. Garrahan, J. Phys. Chem. B **109**, 3578 (2005).
[12] W. Götze and M. Sperl, Phys. Rev. Lett. **92**, 105701 (2004).
[13] K. S. Cole and R. H. Cole, J. Chem. Phys. **9**, 341 (1941).
[14] T. Franosch, M. Fuchs, W. Götze, M. R. Mayr, and A. P. Singh, Phys. Rev. E **55**, 7153 (1997).
[15] W. Götze, J. Phys.: Condens. Matter **2**, 8485 (1990).
[16] M. Fuchs, W. Götze, and M. R. Mayr, Phys. Rev. E **58**, 3384 (1998).
[17] W. Götze, Z. Phys. B: Condens. Matter **56**, 139 (1984).
[18] W. Götze and L. Sjögren, J. Phys.: Condens. Matter **1**, 4183 (1989).
[19] M. Fuchs and T. Voigtmann, Philos. Mag. B **79**, 1799 (1999).
[20] L. Sjögren, Phys. Rev. A **33**, 1254 (1986).
[21] G. Buchalla, U. Dersch, W. Götze, and L. Sjögren, J. Phys. C **21**, 4239 (1988).
[22] A. P. Singh, G. Li, W. Götze, M. Fuchs, T. Franosch, and H. Z. Cummins, J. Non-Cryst. Solids **235-237**, 66 (1998).
[23] B. Ruffle, C. Ecolivet, and B. Toudic, Europhys. Lett. **45**, 591 (1999).
[24] A. Brodin, M. Frank, S. Wiebel, G. Shen, J. Wuttke, and H. Z. Cummins, Phys. Rev. E **65**, 051503 (2002).
[25] S. Wiebel and J. Wuttke, New J. Phys. **4**, 56 (2002).
[26] H. Cang, J. Li, H. C. Andersen, and M. D. Fayer, J. Chem. Phys. **123**, 064508 (2005).
[27] W. Götze and T. Voigtmann, Phys. Rev. E **61**, 4133 (2000).
[28] L. Sjögren, in *Basic Features of the Glassy State*, edited by J. Colmenero and A. Alegría (World Scientific, Singapore, 1990),

pp. 137–151.
[29] M. Sperl, J. Non-Cryst. Solids (to be published).
[30] V. Krakoviack, C. Alba-Simionesco, and M. Krauzman, J. Chem. Phys. **107**, 3417 (1997).
[31] V. Krakoviack and C. Alba-Simionesco, J. Chem. Phys. **117**, 2161 (2002).
[32] H. Z. Cummins, J. Phys.: Condens. Matter **17**, 1457 (2005).
[33] P. K. Dixon, L. Wu, S. R. Nagel, B. D. Williams, and J. P. Carini, Phys. Rev. Lett. **65**, 1108 (1990).
[34] M. Sperl, Phys. Rev. E **71**, 060401(R) (2005).
[35] W. van Megen, T. C. Mortensen, S. R. Williams, and J. Müller, Phys. Rev. E **58**, 6073 (1998).